International Journal of Thermofluid Science and Technology (2020)
Volume 7, Issue 4, Paper No. 070401
https://doi.org/10.36963/IJTST.2020070401
Research Article

Heat and mass transfer modeling during laminar condensation of non-cryogenic downward fluids flow in a small vertical tube

Youssef Belkassmi[1], Lahoucine Elmaimouni[1], Abdessamade Rafiki[1], Kamal Gueraoui[2], Najem Hassanain[3]

[1]*ERMAM, Ibn Zohr University, Polydisciplinary Faculty ,Ouarzazate, Box 638, Morocco,*
[2]*MSME, Mohammed-V University, Faculty of Sciences, Rabat, Morocco.*
[3]*Group of Semiconductors and Environmental Sensor Technologies-Energy Research Center, Faculty of Science, Mohammed V University, B. P. 1014, Rabat, Morocco.*

Received: 24 July 2020; Received in revised form: 18 August 2020; Accepted: 1 September 2020;
Published online: 18 September 2020

Abstract

The purpose of this paper is to investigate mass and heat transfer in the process of film condensation of vapor-air mixture for non-cryogenic fluids flow in a small vertical tube. A two-phase mathematical model is developed to model the mixture and liquid film. The governing equations for mixture and liquid-film have been resolved using a numerical method. Furthermore, this phenomenon analyzed is linked to a steady-state. Therefore, the development of numerical codes allows us to investigate the effect of implicated parameters on this phenomenon. Ethanol and methanol as non-cryogenic typical working fluids are realized for a good understanding of the heat and mass transfer mechanism during condensation. In this way, several effects of influencing parameters were examined. The predicted results showed a good agreement with experimental data.

Keywords: Condensation; Heat transfer; Mass transfer; Fluid flow; Vertical tube; Non-cryogenic fluids.

1. Introduction

The mass and heat transfer during condensation is important for many heat exchanger applications, such as air conditioning, generation of electricity, refrigeration, reactor safety, aerospace, desalination, etc[1]. Indeed, the first theoretical model describing this phenomenon was conducted by [2] in the event of laminar film condensation of pure stagnant steam on a vertical plate. Therefore, several studies on condensation in different systems were then carried out. The reader can find a bibliographic synthesis in this domain in the references [3-4]. However, many studies on non-cryogenic fluids flow condensation in different systems have been realized. Indeed, non-cryogenic fluids flow condensation in small tubes/channel is promising in industrial use [5]. So far, numerical studies focusing on

Corresponding e-mail: y.belkassmi@uiz.ac.ma (Youssef Belkassmi)

heat and mass transfer characteristics of non-cryogenic fluids process are relatively recent [6-9]. Furthermore, studies with small vertical/horizontal tubes are limited. In both cases, theoretical and experimental condensation studies lead to select some types of parameters, namely: parameters related to the nature of the steam undergoing condensation (pure, mixed, or mixed with a non-condensable vapor). Parameters characterizing the nature and geometry of the wall (tube, channel, vertical, inclined, single wall, or covered with a porous layer). And the parameters relating to the condensation mode (film, droplets, etc.).

Nomenclature

Cp	Specific heat $[J.K^{-1}.kg^{-1}]$	**Grec**	
D	Mass diffusivity $[m^2s^{-2}]$	δ	Film thickness $[m]$
d	Tube diameter [m]	δ^*	Dimensionless film thickness
g	Gravitational acceleration $[m.s^{-2}]$	λ	Thermal conductivity $[W.K^{-1}]$
h_{fg}	Latent heat of condensation $[J.kg^{-1}]$	η	Transformed radial coordinate
h_x	Local heat transfer coefficient $[W.m^{-2}.K^{-1}]$	μ	Dynamic viscosity $[Pa.s]$
$\dot{m}_0$	Mass flow rate $[kg.m^{-1}.s^{-1}]$	ρ	Mass density $[kg.m^{-3}]$
M_V	Mass of vapor	**Subscripts**	
m_I	Condensing mass flux $[kg.mol^{-1}k^{-1}]$	L	Liquid film
Nu	Overall Nusselt number	v	Vapor
P	pressure	w	wall
q	heat flux $[W.m^{-2}]$	0	Inlet
Re	Reynolds number	b	Bulk
r	Coordinate normal to the tube	m	mixture
Sh	Sherwood number	I	Interface
T	Temperature $[K]$	n	Iteration
u	Radial velocity $[m.s^{-1}]$		
v	Transversal velocity $[m.s^{-1}]$		
w	Fraction of vapor		
x	Coordinate along the tube $[m]$		

Concerning a vertical tube, a condensation model by forced convection for laminar flow was reported by [10]. This model constitutes a contribution to contribute to understanding the process of laminar mixed-convection condensation with a non-condensable gas. [11] studied a laminar liquid film. They considered an isothermal wall and there theoretical model elaboration was considered at the interface the evolution of the shear stresses. [12] performed a laminar mixed convection condensation of mixture numerically. A non-condensable gas was taken into account. Based on two-dimensional equations and two-phase boundary layer, they investigate a thermal balance at the interface to calculate film thickness. In the same context, a two phase boundary layers was investigated by [13]. The forced convection of condensation of refrigerants R123 and R134 their mixture was studied by [14] between two horizontal plates. The coupled equations of mass conservation, the species, momentum and energy are investigated in two phases flow model. The study of

turbulent film condensation was conducted by [15] inside a vertical tube in which with isothermal walls.

The saturated vapor of R123, R134a then the mixture of R134a-R123 is studied. Coupled boundary layer equations of film and mixture were employed [16-20]. All these studies concern two-phase models to study mass and heat transfer for mixed-convection condensation. This model concerned a vertical tube, in the case of mixture turbulence [17], an inclination angle of the tube on simultaneous condensation [18, 21] and a study outside of a smooth tube. Result conducted shows that the heat transfer coefficient increases depending on the mass flow rate. Then, the pressure drop along the tube increased with the seam way of heat transfer. In the study of [21], the pressure drop of condensation was numerically investigated inside a smooth tube. This study used 8.38 mm of inner diameter and 1.48m of length. The fluid of condensing was R134a at 40 ℃ saturation temperature. Among the results, the effect of inclination angle on void fraction and pressure drop at high mass fluxes became negligible.

In the research of [19], an experimental study for R170 was conducted. This study concerns a condensation in the horizontal tube with 4mm inner diameter. They examined saturation pressure (from 1MPa to 2.5 MPa) and mass flow effects on heat transfer. They compared various well-known correlations with experimental data. In addition, the [22] correlation can accurately predict the experimental pressure drop with a main absolute relative deviation is less than 18 ℃. Numerical simulation of film condensation in a vertical channel performed by [23]. In this study, an analytical model of film condensation is conducted with consideration of the effect of vapor flow in the Nusselt model [2]. Results show that as the inlet vapor velocity increases, the film of condensate tends to be thinner. This was explained by the increase of vapor the wall heat flux the increases of shear stress. [24] reported an experimental study for the condensation of steam on square wire wrapped on a horizontal copper tube.

An analytical solution for the laminar film in the case of simplified steady-state equations for pure water vapor was conducted by [25-26]. Thy interested in film respectively in an inclined and horizontal tube. [27] developed an equation that relates the mixture-liquid interface parameters and stream parameters based on the thermodynamic analysis. They also presented a forced convection film condensation on the outside surface of a horizontal tube. Results indicate that increases in the mass fraction of the noncondensable gas in the stream reduce the heat flux. Recently, a numerical study of laminar film condensation was conducted by [7]. This study concerns a case of pure vapor in an isothermal vertical tube. However, they based on the assumptions taken into account in the Nusselt study [2]. Besides, they simplified the Navier-Stokes equations for obtained the equation of liquid film thickness for film-wise condensation on fluted surface. Curvature variation effects on a condensing were investigated based on liquid film thickness equation. An experimental study of condensation in a horizontal low-finned tube was investigated by [28]. The condensate retention between pure steams compared with that of fins was found lower due to lower surface tension. They noted also, that it resulted in vapor-side enhancement around 3, further 50% of the heat transfer over most of the range of data. In the literature, other authors were interested by the study of heat and mass transfer in vertical tube among them we cite [29]. Also, mass and heat transfer for water film simulated numerically by many authors such [30-36].

To the author's best knowledge; there are no published experimental studies on laminar film condensation from vapor-gas mixtures in small vertical tube. Thus, this study is

going to develop theoretically model of heat and mass transfer for laminar condensation of non-cryogenic downward fluids flow in small vertical tube.

The manuscript is organized as follows: Section Model presents the mathematical model. Section Method proposed method and model validation. Section Results reports the results and physical discussions. The final section presents the conclusions.

2. Problem Formulation

Fig.1 shows geometry under consideration with the boundary conditions. The tube dimensions are width d=2R=0.005m and length L=2m. The mixture vapor-gas flow enters the tube with a uniform inlet temperature T_0, uniform velocity u_0, and uniform pressure P_0. For the walls Dirichlet condition was chosen.

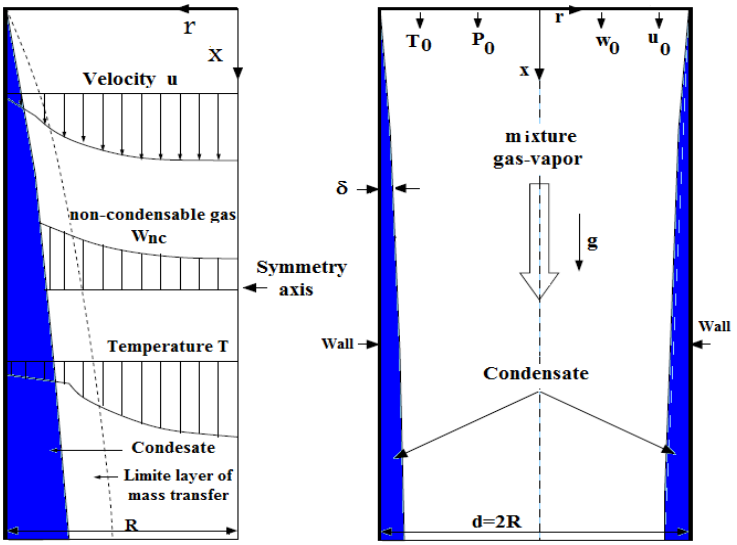

Fig. 1. Geometry with the boundary conditions.

Assumptions and Governing Equations

The following assumptions have been formed in the development of the governing equation. The liquid and gas flows are laminar and the flow is two-dimensional with symmetries ax. It implies that the flow velocity has only two components: u(axial) and v(radial) and that all the physical quantities involved in the problem depend only on the axial and radial coordinates. Condensate film is impermeable to incondensable gas and Interface liquid and vapor-gas mixture is in the thermodynamic equilibrium. Humid air is an ideal mixture of Methanol/Ethanol vapor. It is considered an ideal gas. For relatively low pressures, the equation of state of ideal gases can then be applied $P_k = (\rho_k RT)/M_k$. The fluids are viscous Newtonian. The Newtonian fluid hypothesis is justified for most fluids and allows us to write that the tangential shear stress is proportional to the transverse velocity gradient $\tau = \mu \partial u / \partial r$. The approximations of the boundary layer are assumed valid for liquid film and gas mixture. This hypothesis allows the elimination of axial diffusion terms $\partial^2 / \partial x^2$ in the transfer equations and the radial pressure gradient which leads to parabolic equations. The liquid film is governed respectively by an equation of continuity, momentum equation, and energy equation.

$$\frac{\partial}{\partial x}\left(\rho_L.u_L\right)+\frac{1}{r}\frac{\partial}{\partial r}\left(r\rho_L.v_L\right)=0 \tag{1}$$

$$\frac{\partial}{\partial x}\left(\rho uu\right)_L+\frac{1}{r}\frac{\partial}{\partial r}\left(r\rho uv\right)_L=-\frac{dP}{\partial x}+\frac{1}{r}\frac{\partial}{\partial r}\left(r\mu\frac{\partial u}{\partial r}\right)_L+\rho_L g \tag{2}$$

$$\frac{\partial}{\partial x}\left(\rho uC_PT\right)_L+\frac{1}{r}\frac{\partial}{\partial r}\left(r\rho vC_PT\right)_L=\frac{1}{r}\frac{\partial}{\partial r}\left(r\lambda\frac{\partial T}{\partial r}\right)_L \tag{3}$$

The mixture vapor-gas is governed by the same equation as the liquid plus an equation of species as follows:

$$\frac{\partial}{\partial x}\left(\rho u\right)_m+\frac{1}{r}\frac{\partial}{\partial r}\left(r\rho v\right)_m=0 \tag{4}$$

$$\frac{\partial}{\partial x}\left(\rho_m.u_m.u_m\right)+\frac{1}{r}\frac{\partial}{\partial r}\left(r\rho_m.u_m.v_m\right)=-\frac{dP}{\partial x}+\frac{1}{r}\frac{\partial}{\partial r}\left(r\mu_m\frac{\partial u_m}{\partial r}\right)+\left(\rho_m-\rho_0\right)g \tag{5}$$

$$\frac{\partial}{\partial x}\left(\rho_m u_m C_{Pm}T_m\right)+\frac{1}{r}\frac{\partial}{\partial r}\left(r\rho_m v_m C_{Pm}T_m\right)= \frac{1}{r}\frac{\partial}{\partial r}\left(r\lambda_m\frac{\partial T_m}{\partial r}\right)+\frac{1}{r}\frac{\partial}{\partial r}\left[\rho D(C_{pv}-C_{pa})T_m\right]\frac{\partial w}{\partial r} \tag{6}$$

$$\frac{\partial}{\partial x}\left(\rho_m u_m W_m\right)+\frac{1}{r}\frac{\partial}{\partial r}\left(r\rho_m v_m W_m\right)=\frac{1}{r}\frac{\partial}{\partial r}\left(r\rho_m D\frac{\partial w}{\partial r}\right) \tag{7}$$

Interface Boundary Conditions

Inlet conditions at (x = 0):

$$x=0\ ,\ T_m=T_0\ \ ,\ w_m=w_0\ ,\ P_m=P_0 \tag{8}$$

At (r=0):

$$\left(\partial u/\partial r\right)_m=\ \ ,\ \left(\partial T/\partial r\right)_m=\ \ ,\ \left(\partial w/\partial r\right)_m=\ \ ,\ v_m=0 \tag{9}$$

Wall condition at (r = R):

$$u_L=v_L=0\ \ ,\ \ T=T_w \tag{10}$$

Continuities at the interface ($r=R-\delta$) for velocity and temperature:

$$u_I(x)=u_{m,I}=u_{L,I} \tag{11}$$

$$T_I(x)=T_{m,I}=T_{L,I} \tag{12}$$

For a Newtonian fluid no slip is assumed:

$$\tau_I=\mu_m\left(\frac{\partial u}{\partial r}\right)_{m,I}=\mu_m\left(\frac{\partial u}{\partial r}\right)_{L,I} \tag{13}$$

The velocity of air-vapor mixture:

$$v_I=-\left(\frac{D_m}{1-w_I}\right)\left(\frac{\partial w}{\partial r}\right) \tag{14}$$

Heat balance:

$$\lambda_L\left(\frac{\partial T_L}{\partial r}\right)_I=-\lambda_m\left(\frac{\partial T_m}{\partial r}\right)_I+h_{fg}\ \dot{m}_I \tag{15}$$

The (Eq.15) can be expressed as follow:

$$q_I = q_s + q_l = \left(\lambda_L \frac{\partial T_L}{\partial r} \right)_I + h_{fg} \dot{m}_I \tag{16}$$

This (Eq.16) presents the total heat transfer which equals the sum of sensible heat and the latent heat. The mass fraction of vapor in the mixture can be calculated using the flowing equation (Eq.17).

$$w_I = \frac{MvP_{v,I}}{M_a \left(P_m - P_{v,I} \right) + MvP_{v,I}} \tag{17}$$

Mixture Properties

Assuming ideal gas behaviors, the total pressure P_m at any point within the vapor–gas mixture is given by the sum of the vapor and gas partial pressures:

$$P_m = Pv + Pa \tag{18}$$

The temperature of the vapor and noncondensable gas are assumed to be equal $T_g = T_v$.

$$\rho_v = \frac{m_v p_v}{RT_v} \tag{19}$$

$$\rho_a = \frac{m_a p_a}{RT_v} \tag{20}$$

The total mixture density can be defined as,

$$\rho_m = \rho_v + \rho_a \tag{21}$$

Where ρ_v and ρ_a are the local vapor and air density, and ρ_m is the local mixture density. Assuming the vapor-gas mixture is incompressible; the local mass fraction of the vapor and air gas can be defined as (Eq.22) where $w_v + w_a = 1$.

$$w_v = \frac{\rho_v}{\rho_m}; w_a = \frac{\rho_a}{\rho_m} \tag{22}$$

By using the above equations we get,

$$p_v = \frac{M_a w_v}{\left(1 - w_v\right) M_v + w_v M_a} p_m \tag{23}$$

Since, the partial pressure of non-condensable gas can be written similarly as,

$$p_g = \frac{M_v \left(1 - w_v\right)}{\left(1 - w_v\right) M_v + w_v M_a} p_m \tag{24}$$

Then, the molar fraction of the vapor components, at the interface, can be defined as,

$$w_{v,I} = \frac{p_{v,I} M_v}{M_a \left(p_{a,I} - p_{v,I} \right) + M_v p_{v,I}} \tag{25}$$

Heat and Mass Transfer Parameters

Bellow, we define a local Nusselt and Sherwood numbers along of interface relating respectively to the heat and mass transfer coefficient:

$$Nu_x = \frac{h_T d_h}{\lambda_m} = \frac{q_I d_h}{\lambda_m (T_I - T_b)} \tag{26}$$

$$Sh_x = \frac{h_{M,x} d_h}{(D_v)} = \frac{\dot{m}_I (1 - w_I) d_h}{\rho_m (D_v)(w_I - w_b)} \tag{27}$$

The mass flow rate of the condensation is expressed as:

$$\dot{m}_I = \frac{\rho_m D_v}{1 - w_I} \cdot \frac{\partial w}{\partial r} \tag{28}$$

Besides, the overall mass balance must be conserved which means mass conservation, therefore:

$$\dot{m}_0 / 2 = \int_0^{d-\delta} (\pi r \rho u)_m \, dr + \int_0^x (\pi r \rho v)_I \, dx \tag{29}$$

A condensing rate can also give an idea of the performance of condensation in the tube (Eq.30). Therefore, a non-dimensional number is introduced as follow:

$$M_r = \int_0^x \dot{m}_I dx / \dot{m}_0 \tag{30}$$

With $\dot{m}_0$ and $\dot{m}_I$ are respectively the mass debit of vapor and the condensate mass rate. $\dot{m}_0 [kg.s^{-1}]$ defined as, $\dot{m}_0 = \pi (d - \delta_0)^2 \rho u_0$.

According to the results of the bibliographic review, several studies have considered that the thermodynamic properties are constant. However, they are not. Therefore, in this study, the thermodynamic properties of the vapor-gas and liquid film mixture are considered as a function of temperature. These properties are calculated using correlations reported in the literature.

3. Method

The parabolic systems equations (1)-(7) with the appropriate boundary conditions were transformed into algebraic equations system using a finite differences method. An implicit scheme is used. The problem is approached by making appear beforehand a form common in to all the equations, which makes it possible to apply it on all the equations. A non-uniform mesh is used while increasing the number of nodes at the inlet and at the interface where the gradients are important. Each grid step is increased by a fixed percentage α in an axial direction and β in a radial direction. After discretization, the nonlinear equations obtained are coupled and depend on the values of velocities and radial coordinates at the considered nodes. Thomas algorithm [37] has been implemented to solve the system equation. A proposed method by Raithby and Schneider [38] has been implemented to velocity and correct pressure.

Resolution Procedure

To solve the system of equations some steps were followed:

- Evaluate the initial values of element I;
- Assume the pressure gradient dp / dx and thickness film δ_x;
- Calculate the radial velocity of vapor and liquid film;

- Integrate the continuity equation to calculate the transversal velocities;
- Calculate the temperatures in the liquid film and mixture phase;
- Calculate the error mass of both liquid film and mixture;
- Approximate liquid film thickness equation (31) and pressure gradient equation (32) using the numerical method as:

$$\delta_x^{n+1} = \delta_x^n - er_L^n \frac{\delta_x^n - \delta_x^{n-1}}{er_L^n - er_L^{n-1}} \tag{31}$$

$$\frac{dp}{dx}^{n+1} = \frac{dp}{dx}^{n} - er_m^n \frac{\left(\frac{dp}{dx}\right)^n - \left(\frac{dp}{dx}\right)^{n-1}}{er_m^n - er_m^{n-1}} \tag{32}$$

- Correct pressure and velocity [37].
- Check mass satisfaction.
- If the satisfaction of the mass is verified, pass to the convergence criterion equation (33) for (T, u and w)

$$\frac{\max\left|\phi^n - \phi^{n-1}\right|}{\max\left|\phi^n\right|} < 10^{-5} \tag{33}$$

- If it is checked between two successive iterations for all the nodes of the line, then we go the next step. If not, the process must be repeated.
- Obtain the data of (I+1).
- Evaluate the new values of the variables dependent on the thermodynamic properties of the fluid.
- Obtain the data of the tube.

Stability Mesh

To ensure the stability of our grid and that the results are grid independent server tests were carried out. Therefore, we have compared the total heat transfer for different values of I, J and K. In light of those results, the calculations were performed with $131\times(81+31)$ grids this is an optimum mesh of this study. For this reason, the grid distribution adopted in this study consists of 31, nodes, in the transverse direction of the liquid region, of the liquid region, 81 and 131 nodes respectively in the transverse direction of the mixture region and in the axial direction. In another way, we transformed the cylindrical coordinates into a coordinate system η, in such a way that $\eta = 0$ corresponds to center line $\eta = 1$ corresponds to the liquid-mixture interface $\eta = 2$ corresponds to the wall. The equations of this change are:

$$\eta_m = r \quad for \quad (R-\delta) \le r \le R \tag{34}$$

$$\eta_L = 2-(R-r)/\delta \quad for \quad 0 \le R-\delta \tag{35}$$

The sensitivity of the numerical model was conducted for the dimension of the mesh to determine the optimal mesh. Some dimensions of grids have benne used to calculate the Nusselt number equation (26). Indeed, it's the most severe test. The calculation of the error for the grid shows that the error does not exceed 5% in the case $NI = 141, NJ = 81, NL = 31$, consequently, the grid $141\times(81+31)$ mesh was used for following our study. Table.1 shows the comparing number of local Nusselt at the interface for a different mesh with A, B, C, and

D corresponding respectively to $131\times(51+21)$, $131\times(81+21)$, $141\times(51+21)$ and $141\times(81+31)$ dimensions.

Table.1. Local Nusselt number for various grid arrangements at the interface (P_0=1atm, T_0=25 ℃, Re_0=500).

x/d	A	B	C	D
1.511	142.885	149.994	149.557	157.786
4.581	91.883	95.104	87.608	90.494
20.878	57.873	59.115	57.667	58.874
58.766	40.300	40.829	39.840	40.275
102.459	31.479	31.774	31.406	31.576
152.212	25.1694	25.343	25.198	25.243
230.236	18.820	18.905	18.690	18.671

Model and Code Validation

To further check the adequacy of our model and code, the results of the present model were first compared with those of [39] for humid air. Fig.2 shows the evolution of sensitive Nusselt number according to input Reynolds number for $P_0 = 1atm$, $T_0 = 60^\circ C$, $\Delta T = 55^\circ C$. We note that the relative error between the present predictions and those of [39] is less than 3%. The discrepancies shown are essentially due to the thermophysical properties used in the two studies. It follows that the model and the proposed numerical code are considered to be suitable for this purpose.

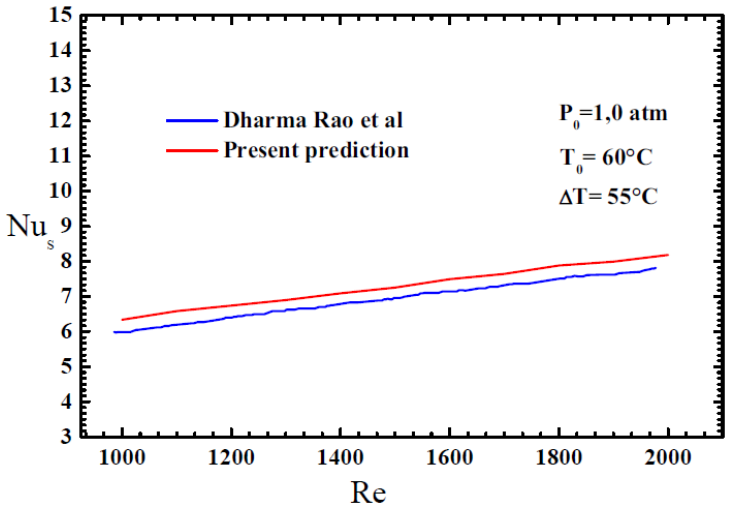

Fig. 2. Sensitive Nusselt number versus the Reynolds number.

4. Results and Discussion

The graph in Fig.3 uses film thickness to examine the effect of changing W_0 for the same Re_0, ΔT, and P_0 for both fluids Ethanol and Methanol. This can be explained by the

fact of the non-condensable gas accumulating near to interface which limits the heat transfer and consequently the deprivation of methanol/ethanol vapor condensation. It shows that the film thickness increase when W_0 is increased. This trend is in conformity with the detrimental effect on heat transfer of increasing quantities of air non-condensable. For 30% of Methanol and Ethanol vapor, the condensation rate is highest. And the effect on the film thickness of increasing W_0 is more pronounced for methanol compared to ethanol.

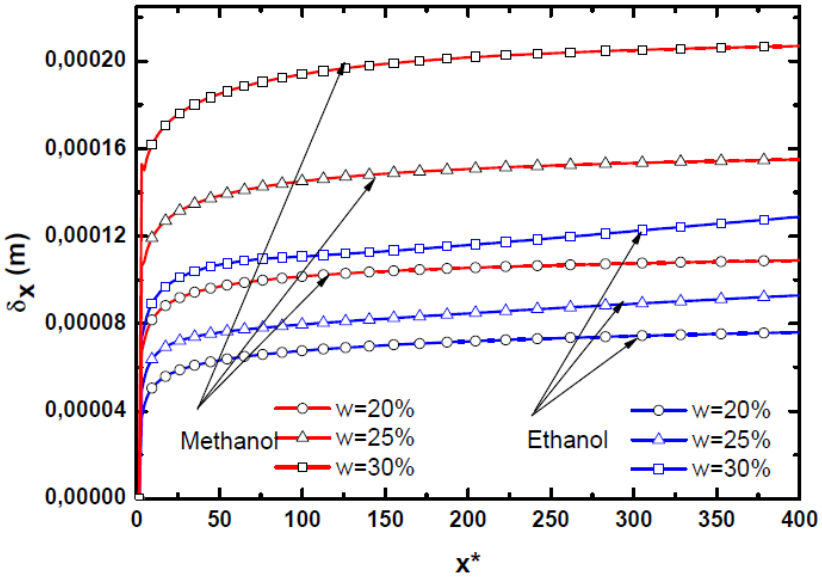

Fig. 3. Thickness film for three vapor fraction values, $\Delta T = 20^{\circ}C, P = 1atm, \mathrm{Re}_0 = 800$

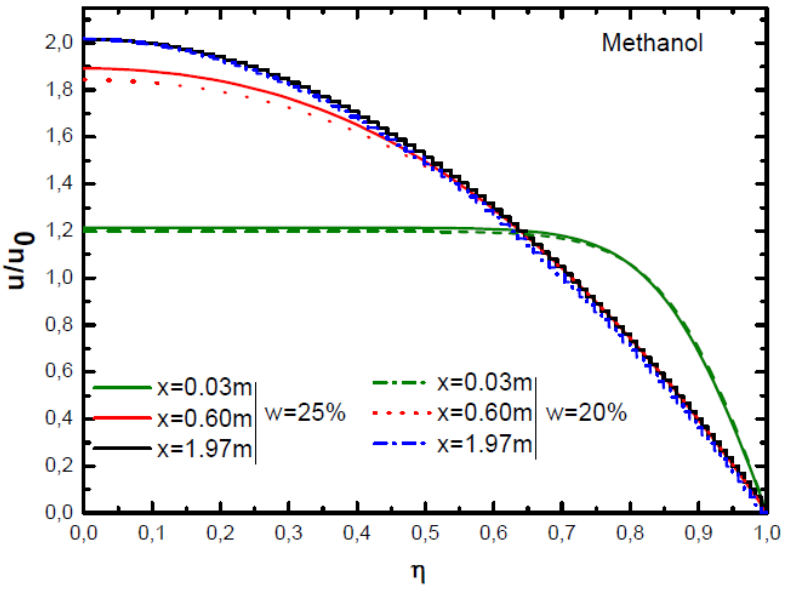

Fig. 4. Dimensionless velocity of Methanol for $\eta \in [0,1], \Delta T = 20^{\circ}C, P = 1atm, \mathrm{Re}_0 = 800$

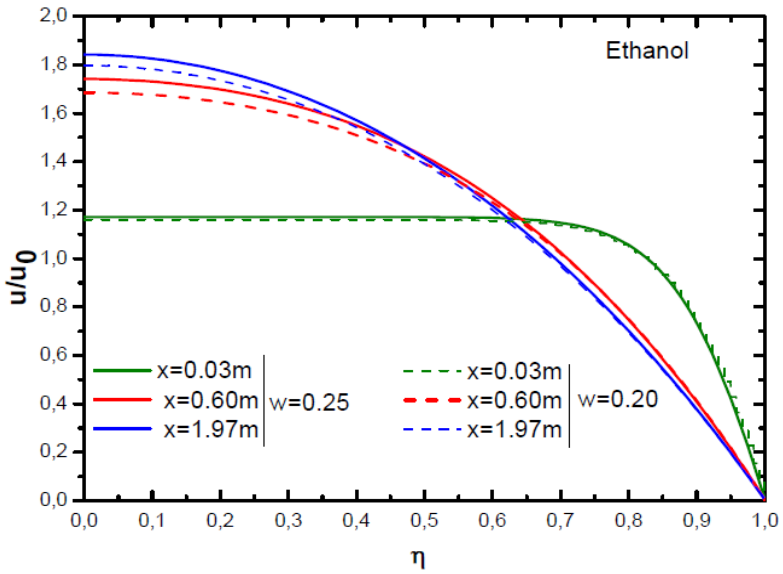

Fig. 5. Dimensionless velocity of Ethanol for
$\eta \in [0,1], \Delta T = 20^{\circ}C, P = 1atm, \mathrm{Re}_0 = 800$

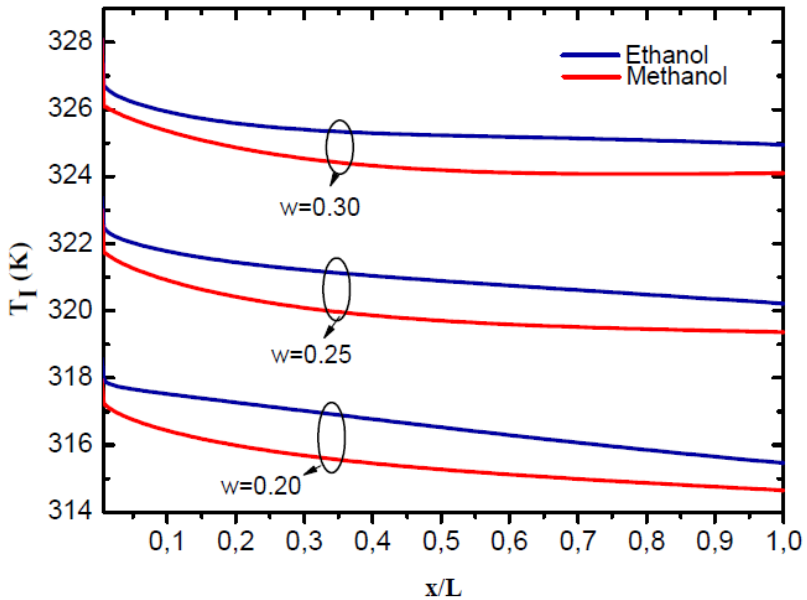

Fig. 6. Interfacial temperature liquid-mixture for three fraction values
$\Delta T = 20^{\circ}C, P = 1atm, \mathrm{Re}_0 = 1000$

In addition, for the fraction values of 30%, the thickness is relatively pronounced because the thermal resistance near to interface is relatively in regression comparing with 30% case. It also shows that heat transfer is important at the entrance, and increases with the fraction of mixture because the decrease in the fraction of the Methanol/Ethanol vapor W_0, signifies an increase of the air in the mixture. This presence of non-condensable gas (air) decreases considerably the exchange coefficient. Indeed, the air vapor lifted up towards the interface by the movement of the steam, thus offering an obstacle to the transfer of vapor to the condensate film. However, for a fully established state is noticed beyond $x^* = 100$. Thus, for the three values of the vapor fraction chosen. As the Fig.3, axial distributions of

dimensionless film thickness for $\Delta T = 20^{\circ}C$, $\mathrm{Re}_0 = 800$, and Nu_x becomes relatively greater in case of methanol.

The evolution of the longitudinal component of the dimensionless velocity $u^* = u/u_0$ depending on the radial distance for three axial positions ($x = 0.03m$, $x = 0.60m$, $x = 1.97m$) and for different conditions simulation, for Methanol Fig.4 and for Ethanol Fig.5. The profile of the longitudinal component depending on radial distance changes from uniform distribution imposed at the entrance x = 0.03 (m) to the parabolic form characteristic of the flow of poison as the gas flows through the tube x = 0.60 m and x = 1.97 (m).

In Fig.6, the effect of the vapor fraction is represented. This figure shows that mixture-liquid interface temperature is generally decreasing along the tube. This decrease can be explained by the cooling of the walls due to the low temperature imposed on them. Besides, it was noticed that an increase in the vapor mass fraction is directly in proportion to an increase in the inlet mixture temperature and consequently (a decrease in the incondensable gas).

The temperature effect difference is represented in figures (7)-(10) for different values of $\Delta T = T_0 - T_W$. For this effect, we chose three values as follows $\Delta T = 10^{\circ}C, 20^{\circ}C, 30^{\circ}C$.

For this effect the inlet temperature is fixed at $50^{\circ}C$ which means a wall temperatures correspond to $40^{\circ}C, 30^{\circ}C$, and $20^{\circ}C$. These figures show that, for the same values of Reynolds number, P_0 inlet pressure and inlet fraction of vapor w_0, the values of heat transfer Fig.7, film thickness Fig.8, rate of condensate Fig.9 and interfacial temperature Fig.10 do not converge to the same limit at the end of condensation at x/d = 400. The increase of ΔT causes a decrease in parietal temperature, the rate of vapor in the mixture, consequently the increase of the difference between the vapor mass fractions.

This leads to increased temperature gradients, vapor concentration, and the rate of condensation. Along the tube, the Nusselt number decreases as the temperature difference increased for both methanol and ethanol Fig.7. Indeed, as Nu_x reaches values greater than (1), the transfer by convection is active. It decreases along the tube as the mixture progresses. It can be shown that heat transfer is important at the entrance and heat transfer increases with the temperature difference because of the increase in the temperature difference (ΔT) signifies a decrease of wall temperature which leads to a reduction of the interface temperature. In addition, the film thickness allows giving an idea with regard to the performance of the condensation phenomenon. Indeed, in Fig.9 it is noted that the condensed mass flow is important for large temperature values and decreases along the tube from input to output. In addition, this result reveals that for the same values of parameters $P = 1atm$, $W = 62\%$, and $Re_0 = 1000$ methanol (b) has a rate relatively more important.

This observation is corroborated by (Fig.8). Since these parameters reflect the mass transfer. It is remarkable to note that condensate film thickness varies according to a very similar trend with the cumulative condensation rate. Indeed, the thickness reaches respectively for Ethanol (a) and Methanol (b) $\delta = 1.7 \times 10^{-4} m$ and $\delta = 1.45 \times 10^{-4} m$. This is because the reason for phase change phenomena is favored by great temperature difference ΔT.

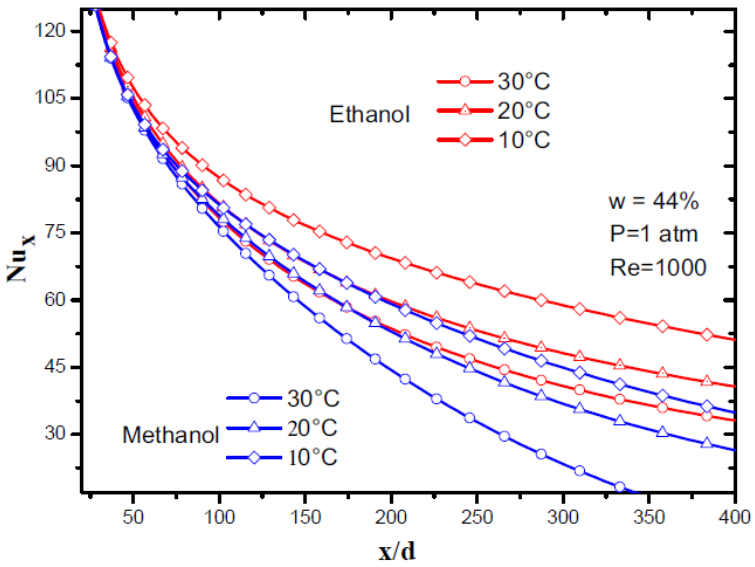

Fig. 7. Local Nusselt number for three temperature gradients, $W = 0.62, P = 1atm, \mathrm{Re}_0 = 1000$.

From the previous figures, Methanol is suitable for condensation comparing to Ethanol case, this is due because of thermal heat capacities that are different and their latent heat. Fig.11 and Fig.12 present graphs of Nusselt number and film thickness for three values of Re_0 for $\Delta T = 20^{\circ}C$, $w_0 = 0.68$ and $P = 1atm$. We notice that the numbers of Nusselt at the interface decreases strongly with the rise of the dimensionless longitudinal coordinate (x/d). Then they tend asymptotically towards a constant value. This evolution results from the definition of the Nusselt number equation (Eq.26).

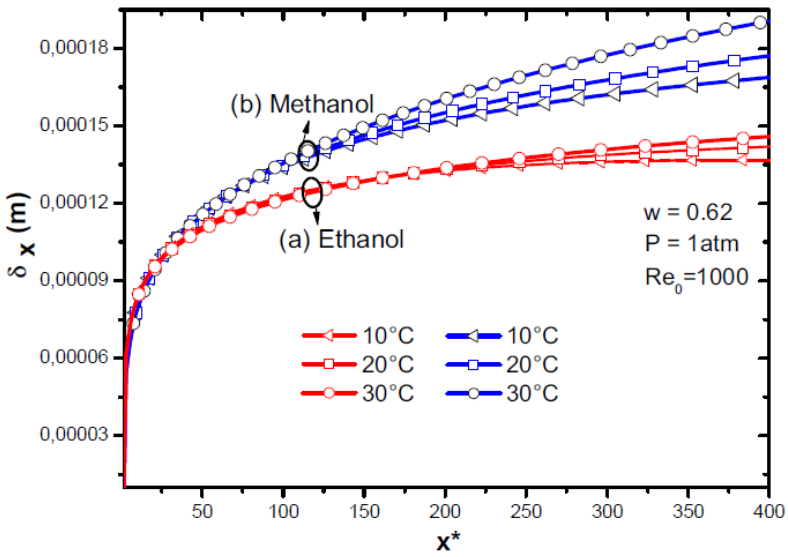

Fig. 8. Condensate film thickness, $W = 0.62, P = 1atm, \mathrm{Re}_0 = 1000$.

As expected, Nu_x increases with inlet Reynolds number, due to the decrease in film thickness, as depicted in Fig.12. However, Fig.11 shows thinner films with increased Re_0 due

to the greater shear force at the interface. Indeed, this is globally due to the ratio of the convective and conductive flow along the tube. In addition, convective transfers are therefore more intense at the entrance of the tube. We also note that the rate of condensation reduces with the rising of Reynolds number. The increase in Reynolds number generates an increase in air vapor accumulated near the interface. As intended, Nu_x increases with Remolds number, due to the decrease in film thickness, as depicted in Fig.11.

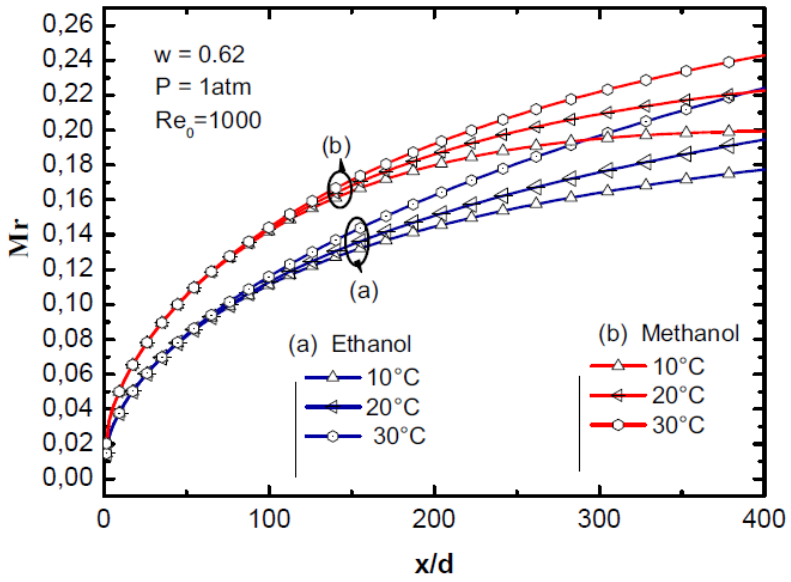

Fig. 9. Rate of mass condensation, $P = 1atm$, $\mathrm{Re}_0 = 100$, $W = 0.68$.

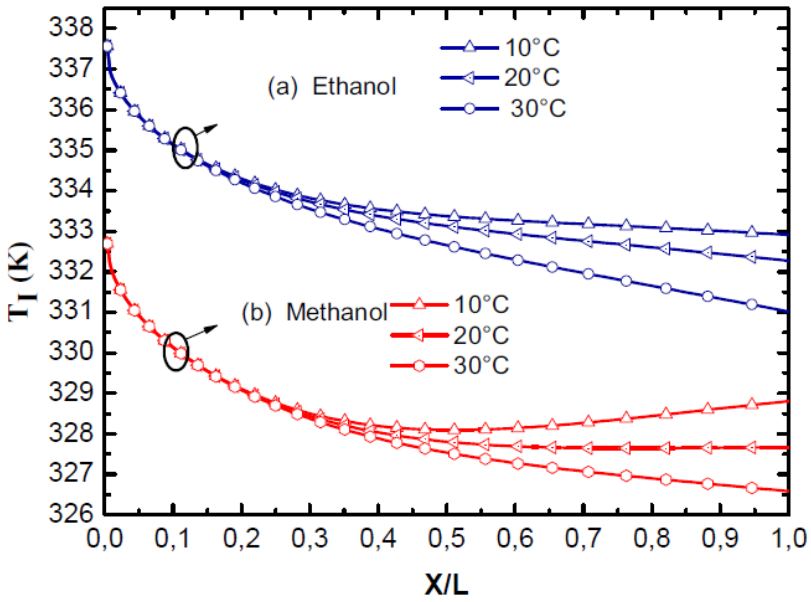

Fig. 10. Interfacial temperature, $\Delta T = 20^{\circ}C, P = 1atm, \mathrm{Re}_0 = 1000.$

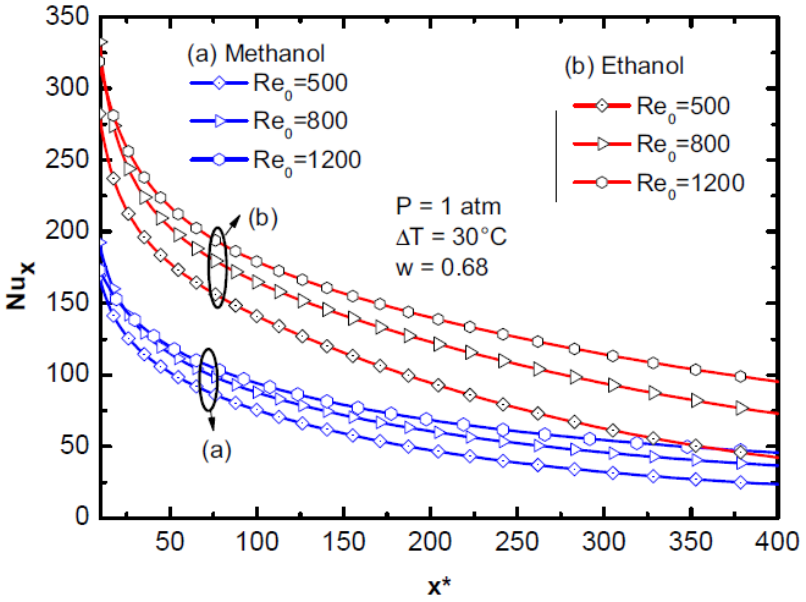

Fig. 11. Local Nusselt number, $\Delta T = 20^{\circ}C$, $P = 1atm$, $W = 0.68$.

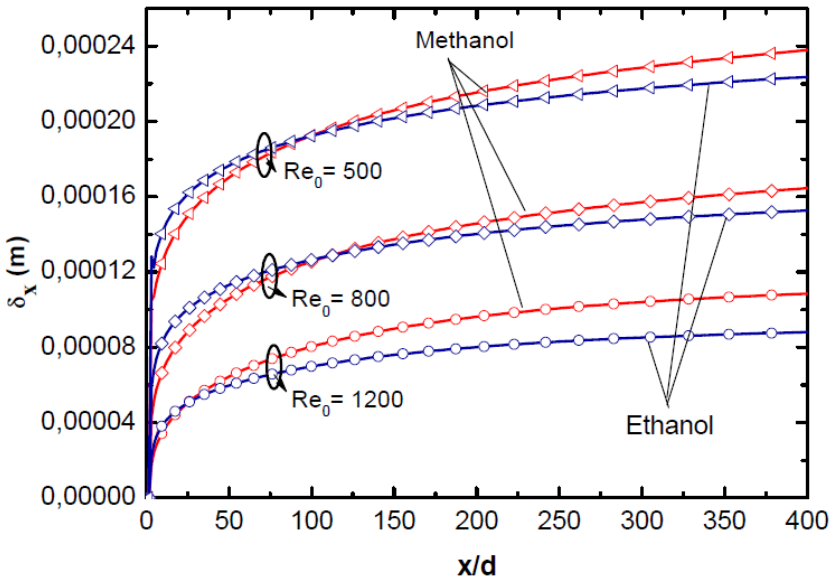

Fig. 12. Film thickness for three Reynolds number values, $\Delta T = 20^{\circ}C$, $P = 1atm$.

Conclusion

Heat and mass transfer in the laminar condensation processes of vapor-air mixture for ethanol and methanol non-cryogenic fluids flow in a small vertical tube has been investigated. Two-phase flows with phase change have been developed. Several effects of varying the inlet parameters have been examined and presented. The main conclusions from this study are synthesized as: Numerical and analytical means have been developed to investigate condensation mass and heat transfer. Along the tube there is a decrease of heat transfer coefficient accompanied by a temperature decrease of the gas mixture. The condensation heat transfer coefficients and the rate of condensation decreases considerably. The mass and heat transfer is improved by large temperature differences, large fractions of vapor, and by low

Reynolds numbers. The condensation process is relatively efficient in the methanol vapor-air mixture compared to ethanol one.

References

[1] Ajmal Shah, Imran Rafiq Chughtai, Mansoor Hameed Inayati, Numerical simulation of direct-contact condensation from a supersonic steam jet in subcooled water. Chinese Journal of Chemical Engineering 18(2010) 577-587. https://doi.org/10.1016/S1004-9541(10)60261-3

[2] W. Nusselt, Die oberflachenkondensation des wasserdampfes, Z. Ver. 303 Deut. Ing 69 (1916) 541–546.

[3] L. Cheng, L. Junming, Laminar forced convection heat and mass transfer of humid air across a vertical plate with condensation. Chinese Journal of Chemical Engineering 19 (2011) 944-954. https://doi.org/10.1016/S1004-9541(11)60076-1

[4] Siow E.C., Ormiston, S.J., Soliman, H.M., Two-phase modelling of laminar film condensation from vapor–gas mixtures in declining parallel-plate channels. International Journal of Thermal Sciences 46 (2007) 458–466. https://doi.org/10.1016/j.ijthermalsci.2006.07.001

[5] Chao Qi, Xiting Chen, Wen Wang, Jianyin Miao, Hongxing Zhang, Experiment and simulation on downward flow condensation of nitrogen in vertical tubes. International journal of heat and mass transfer 146 (202) 118827. https://doi.org/10.1016/j.ijheatmasstransfer.2019.118827

[6] Cheng, L. and L. Junming, Laminar forced convection heat and mass transfer of humid air across a vertical plate with condensation. Chinese Journal of Chemical Engineering 19(9) (2011) 944–954. https://doi.org/10.1016/S1004-9541(11)60076-1

[7] Wang X.W., Leong K.C., Wong T.N., Numerical analysis of different fluted fins for condensation on a vertical tube. International Journal of Thermal Sciences 122 (2017) 359–370. https://doi.org/10.1016/j.ijthermalsci.2017.08.006

[8] UI Yongzhang, TIAN Maoche, ZHANG Linhua, LI Guangpeng and ZHU Jianbin, Three dimensional numerical simulation of convection-condensation of vapor with high concentration air in tube with inserts. Chinese Journal of Chemical Engineering 20 (2012) 686–692. https://doi.org/10.1016/S1004-9541(11)60236-X

[9] Hong-ran Park, Yeongmin Kim, Sung Jo Kwak, Jiyeon Choi, SeungCheol Yang, Moon Hee Han, Dong Kook Kim, Heat and mass transfer of binary distillation in a vertical wetted-wall column. Chemical Engineering Research and Design 128 (2017) 49–58. https://doi.org/10.1016/j.cherd.2017.09.032

[10] Y. Belkassmi, K. Gueraoui, N. Hassanin, Numerical study in condensing of methanol vapor in a vertical tube by mixed convection in the presence of noncondensable gas. Adv Studies Theor Phys 6 (2012) 1065–1076.

[11] Oh S., Revankar S.T., Analysis of the complete condensation in a vertical tube passive condenser. International Communications in Heat and Mass Transfer 32 (2005) 716–727.

https://doi.org/10.1016/j.icheatmasstransfer.2004.10.013

[12] Chin Y., Ormiston S., Soliman H., A two-phase boundary-layer model for laminar mixed-convection condensation with a noncondensable gas on inclined plates. Heat and Mass Transfer 34 (1998) 271–277. https://doi.org/10.1007/s002310050259

[13] Cha'o-KuangChen, Yan-TingLin, Laminar film condensation from a downward flowing steam-air mixture onto a horizontal circular tube. Applied Mathematical Modelling 33 (2009) 1944–1956. https://doi.org/10.1016/j.apm.2008.05.003

[14] P. Panday, Two-dimensional turbulent film condensation of vapors flowing inside a vertical tube and between parallel plates: a numerical approach, International Journal of Refrigeration 26 (2003) 492–503. https://doi.org/10.1016/S0140-7007(02)00162-7

[15] Louahlia H., Panday P.K., Transfert thermique pour la condensation du R123, du R134a et de leurs mélanges en écoulement forcé entre deux plaques planes horizontales: Etude numérique, Rev. Gén. Therm 35 (1996) 615–624. https://doi.org/10.1016/S0035-3159(96)80024-9

[16] Siow E.C., Orimiston S.J., Soliman H.M., A two-phase model for laminar film condensation from steam-air mixtures in vertical parallel plate channels, Heat and Mass Transfer 40 (2004) 365–375. https://doi.org/10.1007/s00231-003-0425-0

[17] Y. Belkassmi, K. Gueraoui, N. Hassanain, A. Elbouzidi, Convective condensation of methanol vapor in presence of a non-condensable gas with turbulent flow in vertical tube, International Review of Mechanical Engineering (IREME) 9 (2015) 167–173. https://doi.org/10.15866/ireme.v9i2.5311

[18] Noori Rahim, Abadi S.M.A., Meyer J.P., Numerical investigation into the inclination effect on conjugate pool boiling and the condensation of steam in a passive heat removal system, International Journal of Heat and Mass Transfer 122 (2017) 1366–1382. https://doi.org/10.1016/j.ijheatmasstransfer.2017.12.093

[19] Zhuang X.R., Gong M.Q., Zou X., Chen G.F., Wu J.F., Experimental investigation on flow condensation heat transfer and pressure drop of r170 in a horizontal tube, International Journal of Refrigeration 66 (2016) 105–120. https://doi.org/10.1016/j.ijrefrig.2016.02.010

[20] S. Koyama, A. Miyara, H. Takamatsu, K. Yonemoto, T. Fujii, Condensation and evaporation of nonazeotropic refrigerant mixrures of r22 and rll4 inside a spirally grooved horizontal tube, the Reports of Institute of Advanced Material Study Kyushu University 1 (1988) 57–75.

[21] S. M. A. Noori Rahim Abadi, Josua P. Meyer, J. Dirker, (2018). Effect of inclination angle on the condensation of r134a inside an inclined smooth tube. Chemical Engineering Research and Design 132, 346–357. https://doi.org/10.1016/j.cherd.2018.01.044

[22] Yan YY, Lin TF, Evaporation heat transfer and pressure drop of refrigerant r-134a in a small pipe, J Heat Mass Transfer 41 (1998) 3072–3083. https://doi.org/10.1016/S0017-9310(98)00127-6

[23] Hyunseung Lee, Gihun Son, Level-set based numerical simulation of film condensation in a vertical downward channel flow, International communications in Heat and Mass Transfer 95 (2018) 171–181. doi.org/10.1016/j.icheatmasstransfer.2018.05.001

[24] Hafiz Muhammad Ali, Muhammad Zeshan Qasim, Muzaffar Ali, Free convection condensation heat transfer of steam on horizontal square wire wrapped tubes, International Journal of Heat and Mass Transfer 98 (2016) 350–358. https://doi.org/10.1016/j.ijheatmasstransfer.2016.03.053

[25] J.A. Howarth, G. Poots, D. Wynne, Laminar film condensation on the underside of an inclined flat plate, Mechanics Research Communications 5 (1978) 369–374. https://doi.org/10.1016/0093-6413(78)90013-7

[26] P.M. Becket, G. Poots, Laminar film condensation on horizontal flat plates, Mechanics Research Communications 2 (1975) 61–66. https://doi.org/10.1016/0093-6413(75)90042-7

[27] Wu X.M., Tong Li, Qianyu Li, Fuqiang Chu, Approximate equations for film condensation in the presence of noncondensable gases, International Communications in Heat and Mass Transfer 85 (2017) 124–130. https://doi.org/10.1016/j.icheatmasstransfer.2017.05.007

[28] H. Ali, M.S. Kamran ,Hafiz Muhammad Ali, F. Farukh, S. Imran, H.S. Wang, Marangoni Condensation of steam ethanol mixtures on a horizontal low-finned tube, Applied Thermal Engineering 117 (2017) 366–375. https://doi.org/10.1016/j.applthermaleng.2017.02.016

[29] Adil Charef, M'barek Feddaoui, Abderrahman Nait Alla, Monssif Najim, Numerical study of humid air condensation in presence of non-condensable gas along an inclined channel, Energy Procedia 139 (2017) 128–133. https://doi.org/10.1016/j.egypro.2017.11.185

[30] M. Feddaoui, H. Meftah, A. Mir, The numerical computation of the evaporative cooling of falling water film in turbulent mixed convection inside a vertical tube, International Communications in Heat and Mass Transfer 33 (2006) 917–927. https://doi.org/10.1016/j.icheatmasstransfer.2006.04.004

[31] G.Manjunatha, C. Rajashekhar, Hanumesh Vaidya, K. V. Prasad, Saraswati, B. B. Divya, Heat Transfer Analysis on Peristaltic Transport of a Jeffery Fluid in an Inclined Elastic Tube with Porous Walls. International Journal of Thermofluid Science and Technology 7(1) (2020) 20070101 https://doi.org/10.36963/IJTST.20070101

[32] B. Sailaja, G. Srinivas , B. Suresh Babu, Free and Forced Convective Heat Transfer through a Nanofluid with Two Dimensions past Stretching Vertical Plate. International Journal of Thermofluid Science and Technology 7(3) (2020) 070302. https://doi.org/10.36963/IJTST.2020070302

[33] M. J. Uddin, A. K. M. Fazlul Hoque, M. M. Rahman , K. Vajravelu, Numerical simulation of convective heat transport within the nanofluid filled vertical tube of plain and uneven side walls. International Journal of Thermofluid Science and Technology 6(1) (2019) 19060101. https://doi.org/10.36963/IJTST.19060101

[34] Bounouar, A., Gueraoui, K., Taibi, M., Driouich, M., Rtibi, A., Belkassmi, Y., Zeggwagh, G., Mathematical and Numerical Modeling of an Unsteady Heat Transfer within a Spherical Cavity: Laser Interaction with Human Skin. International Review of Civil Engineering (IRECE), 9(5) (2018) 209-217. https://doi.org/10.15866/irece.v9i5.14666

[35] Oudrhiri, H., Gueraoui, K., Elbouzidi, A., Sammouda, M., Belkassmi, Y., The Influence of Thermal Grashof Number, Reynolds Number and Schmidt Number on the Behaviour of a

Flow in a Porous Medium. International Review of Mechanical Engineering (IREME), 10(7) (2016) 491-495. https://doi.org/10.15866/ireme.v10i7.9241

[36] M. SAIDI HASSANI ALAOUI, K. GUERAOUI and Y. BELKASSMI, "Numerical and Mathematical Simulation of the Energy Efficiency of Traditional Buildings for Thermal Comfort," 2019 International Conference of Computer Science and Renewable Energies (ICCSRE), Agadir, Morocco, 2019, pp. 1-4, https://doi.org/10.1109/ICCSRE.2019.8807777

[37] S. Patankar, Numerical heat transfer and fluid flow mcgraw-hill, new york (1980).

[38] Raithby G. D., Schneider G. E., Numerical solutions of problems in incompressible fluid flow: treatment of the velocity-pressure coupling, Numer. Heat. Tran. 2 (1979) 417–440. https://doi.org/10.1080/10407787908913423

[39] Dharma Rao V., Murali Krishna V., Sharma K. V., Mohana Rao P. V.J., Convective condensation of vapor in the presence of a non-condensable gas of high concentration in laminar flow in a vertical pipe, International Journal of Heat and Mass Transfer 51 (2008) 6090–6101. https://doi.org/10.1016/j.ijheatmasstransfer.2008.03.027